THE SOUTH POLE-AITKEN BASIN REGION – A NEW GEOLOGICAL MAP. C. M. Poehler[1], C. H. van der Bogert[1], H. Hiesinger[1], M. Ivanov[2] and J.W. Head[3], [1]Institut für Planetologie, Westfälische Wilhelms-Universität, Wilhelm-Klemm-Str. 10, 48149, Münster, Germany, c.poehler@uni-muenster.de, [2]Vernadsky Inst., RAS, Russia, [3]Department of Earth, Environmental and Planetary Sciences, Brown University, Providence, RI 02912 USA.

Introduction: The South Pole-Aitken (SPA) basin is located on the lunar farside, centered at ~53° S, 191° E, and is the largest observable basin on the Moon [1-5]. The largest observable basin on the Moon is the South Pole-Aitken (SPA) basin, centered at ~53° S, 191° E [1-5]. Within the study region we have several hot topic areas such as potentially exposed mantle material [6, 7], sources of volatiles (e.g., pyroclastic deposits [8]), and permanently shadowed regions that may harbor ice or other volatiles [9]. With the SPA basin being the oldest lunar basin, the timing of its formation gives valuable information on the formation and evolution of the lunar crust [8,10]. This makes the region of the SPA basin and in particular the South Pole region targets for several ongoing and future robotic and human missions [e.g., 11-15]

For such missions, detailed studies of the geological history and setting of the region are necessary. Here, we provide a geologic map of the SPA basin region, extending to Orientale basin and including the South Pole area at a scale of 1:500k. An extension of a map of the Apollo basin region [16], our map provides a comprehensive overview of the geology in the region.

Methods: For large-scale mapping, we used the Lunar Reconnaissance Orbiter (LRO) Wide-Angle Camera (WAC) basemap (100 m/pixel). To look at smalleareas and to identify specific features, we then also used Narrow Angle Camera (NAC; 0.5 m/pixel) [17] and Kaguya (10 m/pixel) data. Spectral information was taken from Clementine [18], M^3 [19], and Kaguya MI [20] data. We determined the topographic features using Lunar Orbiter Laser Altimeter (LOLA)/Kaguya merged digital elevation models with a resolution of 59 m/pixel [21] where available. For higher latidues we used LOLA digital elevation products [22, 23]. At the poles we mitigate the effect of low solar illumination angles, which cause significant shadows, by producing hillshade maps with various illumination conditions. We worked according to PLANMAP mapping standards [24], an extension of USGS standards [25].

With the available data we identified different units and features based on their morphological appearance, albedo contrasts and, if applicable, spectral signal. We then established a relative stratigraphy for these units using morphological and stratigraphic evidence. Next, we performed crater size-frequency distribution (CSFD) measurements and determined absolute model ages (AMAs) using the production and chronology functions of [26] to put constraints on the chronology. CSFD measurements were made using CraterTools [27] in ArcGIS, and fit with Craterstats [28]. [26, 29] give detailed descriptions of the technique.

Geology: We cover the full extent of the SPA basin including some of its surrounding in this map. We were able to identify most of the rim of SPA basin, which presents itself best in the elevation data. The visibility of old rim material varies significantly. In the NE part of SPA basin the rim is preserved as a two ring structure. In the South Pole region SPA's rim is obscured by various later impacts We were able to find traces of the outer massif, but most of the inner massif is hidden below younger craters and their deposits.

The whole SPA area is covered in small, sharp-rim craters. Most of these craters are likely linked to the formation of Orientale basin to the E of SPA. As the formation of Orientale basin had a significant effect on SPA basin, we included a large part of Orientale basin in our mapping region.

Acknowledgments: This paper is part of a project that has received funding from the European Union's Horizon 2020 research and innovation programme under grant agreement Nº776276 (PLANMAP) and *N°871149 (GMAP).*

References: [1] Stuart-Alexander (1978) USGS Map I-1047. [2] Spudis et al. (1994) *Science 266*, 1835-1839. [3] Hiesinger and Head (2004) *PLPSC 35*, 1164. [4] Shevchenko et al. (2007) *Solar Sys Res 41*, 447-462. [5] Garrick-Bethell and Zuber (2009) *Icarus 204*, 399-408. [6] Melosh et al. (2017) *Geology, 45*, 1063-1066. [7] Yamamoto et al. (2010*) Nature Geoscience 3*, 533-536. [8] Wilhelms (1987*) USGS SP-1348*, 302. [9] Nozette et al. (2001) *JGR 106*, 23253– 23266. [10] Hiesinger et al. (2012) *LPSC 43*, 2863. [11] Flahaut et al. (2020) *PSS 180*, 104750. [12] Steenstra et al. (2016) *Adv Space Res 58*, 1050–1065. [13] Allender et al. (2018) *Adv Space Res 63*, 692–727. [14] Hiesinger et al. (2019) *LPSC 50*, 1327. [15] Huang et al. (2018) *JGR 123*, 1684 – 1700. [16] Ivanov et al. (2018) *JGR 123*, 2585–2612. [17] Robinson et al. (2010) *Space Sci Rev 150*, 81–124. [18] Pieters et al. (1994) *Science 266*, 1844–1848. [19] Isaacson et al. (2013) *JGR 118*, 369–381. [20] Ohtake et al (2013*) Icarus 226*, 364–374. [21] Barker et al. (2016) *Icarus 273*, 346-355. [22] Smith et al. (2010) *Icarus 283*, 70-91. [23] Smith et al. (2010) *GRL* 37, L18204. [24] wiki.planmap.eu/display/public/D2.1-public. [25] FGDC (2006) FGDC-STD-013-2016. [26] Neukum et al. (2001) *Space Sci Rev 96*, 55–86. [27] Kneissl et al. (2011) *PSS 59*, 1243–1254. [28] Michael and Neukum (2010) *EPSL 294*, 223–229. [29] Hiesinger et al. (2000) *JGR 105*, 29239–29276.

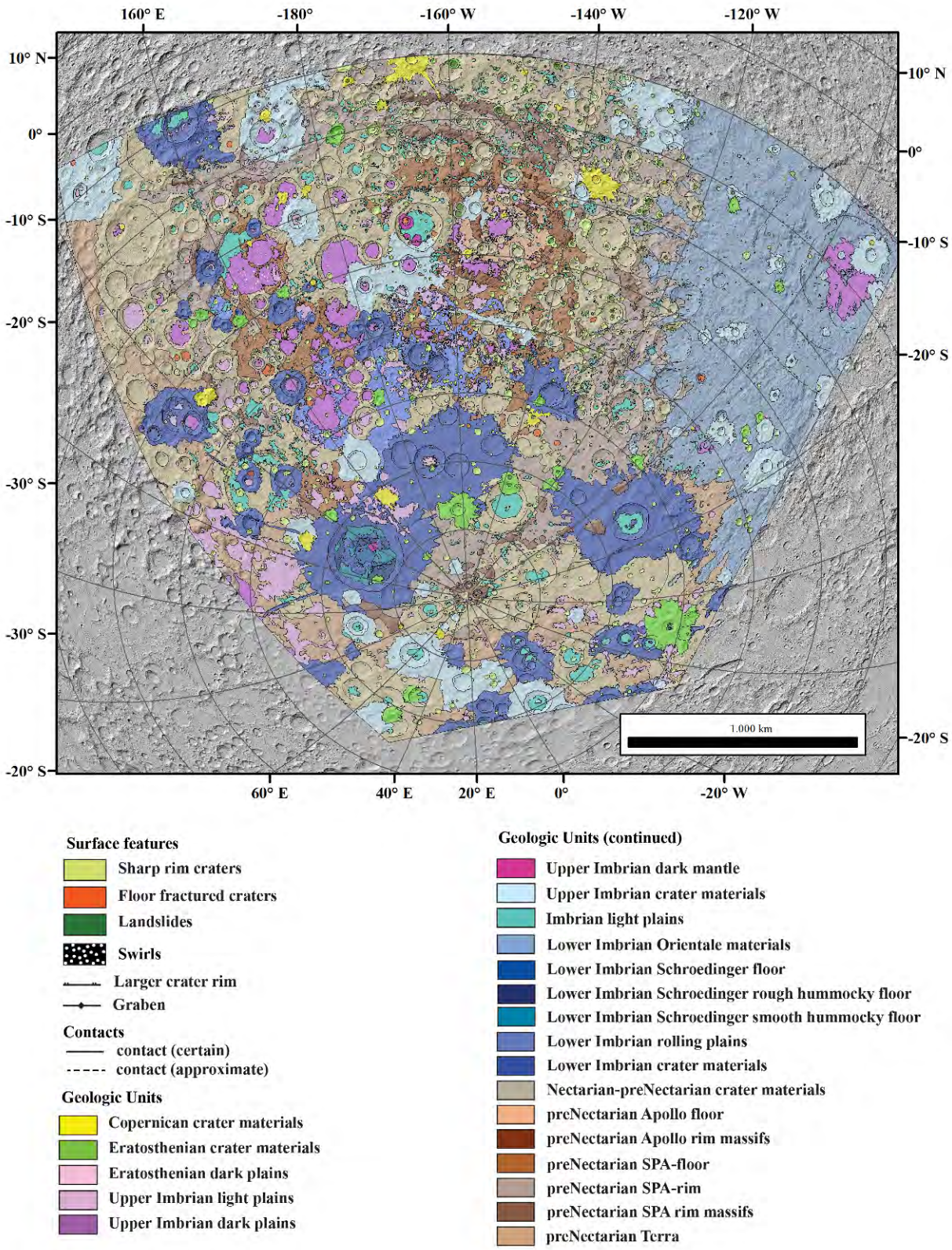

Figure 1. *Preliminary geological map of the lunar South Pole and the South Pole-Aitken basin at a scale of 1:500,000 in Lambert projection centered at 157.5° S and 53° E. The background image is a hillshade map compiled from a LOLA global DEM.*